View metadata, citation and similar papers at core.ac.uk

brought to you by CORE

provided by HKU Scholars Hub

The HKU Scholars Hub The University of Hong Kong 香港大學學術庫

Title	Quantitative comparison of double-stator permanent magnet vernier machines with and without HTS bulks
Author(s)	Liu, C; Chau, KT; Zhong, J; Li, W; Li, F
Citation	IEEE Transactions on Applied Superconductivity, 2012, v. 22 n. 3
Issued Date	2012
URL	http://hdl.handle.net/10722/192183
Rights	Creative Commons: Attribution 3.0 Hong Kong License

Quantitative Comparison of Double-Stator Permanent Magnet Vernier Machines With and Without HTS Bulks

Chunhua Liu, *Member, IEEE*, K. T. Chau, *Senior Member, IEEE*, Jin Zhong, Wenlong Li, and Fuhua Li

***Abstract*—This paper quantitatively compares three types of double-stator flux-modulation permanent-magnet (PM) machines, namely the vernier machine, vernier machine with HTS bulks, and magnetic-geared machine. Due to adopting the double-stator topology, these PM machines achieve the higher energy transmission and power conversion than the single-stator counterparts. Also, the design for the proposed machines are to respectively use the flux-modulation pole, HTS bulk and the flux-modulation ring for modulating the low speed rotating field of the PM rotor and the high speed rotating field of the armature windings, hence obtaining the gear effect for low speed operation. It should be noted that by using the HTS bulks can not only efficiently improve the flux modulation effect of the vernier machine, but also greatly reduce the machine flux leakage. By using the finite-element-method, their performances are compared, hence verifying the validity of the machine design.**

***Index Terms*—Double-stator, finite element method, flux-modulation, high temperature superconductor, magnetic-geared machine, permanent magnet machine, vernier machine.**

I. Introduction

With two sets of armature windings, double-stator permanent-magnet (PM) machines possess the higher torque density and power density, as well as more flexibility for winding connections than the conventional single-stator machines under the same size [1]. PM vernier machines [2]–[4] and magnetic-geared machines [6]–[8] currently attract much attention due to their outstanding flux-modulation feature of providing the high-torque low-speed operation. On the other side, the advent of high-temperature-superconductor (HTS) provides a new way for the machine design, which can greatly improve the performance of the conventional machine [7]–[9].

By taking advantages of the above merits, this paper is purposely to propose three types of double-stator flux-modulation machines, namely the double-stator PM vernier (DSPMV) machine, DS PM vernier HTS (DSPMV-HTS) machine, and DS magnetic-geared (DSMG) machine. The key is to using the flux-modulation pole, HTS bulk, and flux-modulation ring to modulate the low speed rotating field of the PM rotor and the high speed rotating field of the armature windings, hence achieving the gear effect for low speed operation. Also, their DS topologies can effectively benefit the efficiency and energy conversion. In addition, by incorporating the HTS bulks into the DSPMV machine, its flux-modulation ability and performance can be further improved. By using the finite-element-method (FEM), their performances are compared and analysed, which prove the validity of the design of these machines.

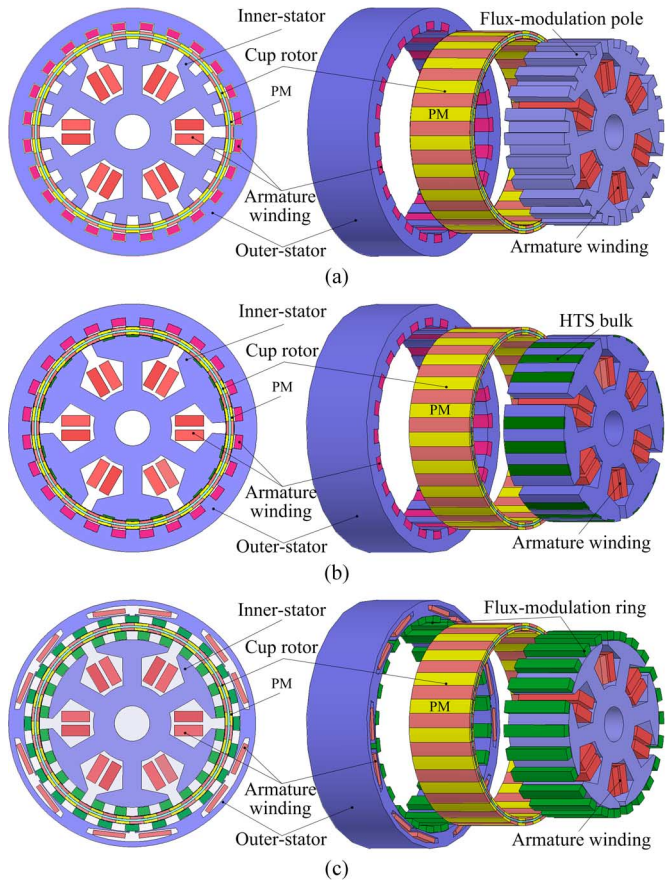

Fig. 1. Proposed double-stator flux-modulation machines: (a) DSPMV, (b) DSPMV-HTS, and (c) DSMG.

II. Machine Design

Fig. 1 shows the configuration of proposed double-stator flux-modulation machines, which has a same cup-rotor for mounting two sets of 22 pole-pair PMs on both inner and outer surfaces.

Manuscript received September 12, 2011; accepted December 13, 2011. Date of publication December 21, 2011; date of current version May 24, 2012. This work was supported by a grant from HKU Small Project Funding (Project Code: 201007176302) and a grant from Research Grants Council (Project Code: HKU 710710E), Hong Kong Special Administrative Region, China.

The authors are all with the Department of Electrical and Electronic Engineering, The University of Hong Kong, Hong Kong (e-mail: chualiu@eee.hku.hk).

Color versions of one or more of the figures in this paper are available online at http://ieeexplore.ieee.org.

Digital Object Identifier 10.1109/TASC.2011.2180870

1051-8223/$26.00 © 2011 IEEE

But they have different double-stator topologies for performing the flux-modulation and energy conversion.

For the rotor structure, since all three machines adopt the cup shape with PMs mounted on both surfaces, the iron core of the rotor can be designed very thin (only 2.4 mm for the proposed machines and about 70% thinner than a comparable machine). Also, the machine magnetic flux path is series, which effectively shorten the magnetic circuit length and hence improve the torque density (about 30% shorter than a comparable machine with the paralleled magnetic path). Moreover, the cup-shaped rotor can make the machine compact and robust, which is suitable for direct-drive application.

For the inner stator topology, all machines adopt 6 embedded slots for accommodating concentrated windings, which can simplify the inner-stator structure and fully utilize the inner stator space, as well as effectively shorten the end winding. In detail, the DSPMV machine utilizes the salient-pole and embedded-slot for performing the flux modulation, whereas the DSPMV-HTS machine uses the HTS bulks for shielding the flux distribution and hence realizing the flux modulation. The configuration of the HTS bulks consists of the HTS bulks, cooling channel around the bulks, vacuum enclosure, and refrigeration source for offering the circulated liquid nitrogen. In addition, the DSMG machine accepts the modulation-ring for accomplishing the flux assignment. Hence, all the inner stators of these machines achieve the similar function of flux modulation. In order to simplify the analysis, the flux-modulation ring of the DSMG machine is treated as the part of the corresponding inner stator or outer stator. And they obey the same tooth-pole arrangement as follow:

$$N_r = N_s - p_s \tag{1}$$

where N_r is the number of rotor PM pole pairs, N_s is the number of flux-modulation poles (HTS bulks or flux-modulation rings), and p_s is the number of armature winding pole pairs [2]–[5]. Hence, the corresponding high-to-low speed ratio G_r is governed by:

$$G_r = \frac{|ip_s + jN_s|}{ip_s} \tag{2}$$

where $i = 1, 3, 5, \ldots$ and $j = 0, \pm 1, \pm 2, \ldots$ [2]–[5]. When $i = 1$ and $j = -1$, the largest space harmonic component can be obtained.

Furthermore, the relationship between the N_s and the p_s can be given as:

$$N_s = m \times p_s \times k \tag{3}$$

where m is the number of winding phases and k is the flux-modulation poles per phase per armature pole. Usually, it has $k = 2, 3, 4, 5, \ldots$.

So, in these machine designs, the parameters are selected for $m = 3$, $p_s = 2$, and $k = 4$. Then, it has $N_s = 24$, $N_r = 22$, and $G_r = 11$. It means that the rotor speed is only 1/11 of that in stator for armature rotating field speed. Thus, when the rotor speed is 200 rpm, the speed of armature rotating magnetic field in stator is scaled up to 2200 rpm.

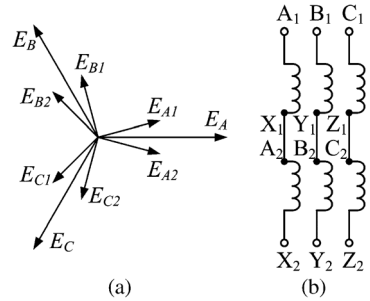

Fig. 2. Series connection of windings: (a) vector diagram and (b) winding.

For the outer stator structure, both of the DSPMV type and DSPMV-HTS machine adopt the same open-slot drum-winding vernier structure for modulating the flux distribution. But the outer stator of the DSMG machine utilizes the fractional-slot concentrated-winding structure and the flux-modulation ring for re-assigning the flux distribution. Since the PM magnetic flux path is designed for series connection, the pole-pair PMs are the same number of 22 on both surfaces. Hence, in order to meet the same ratio G_r of 11, the number of outer stator slots for the DSPMV and DSPMV-HTS machines (or the outer flux-modulation rings for the DSMG machine) is the same as the inner stator salient poles (or the inner flux-modulation rings) N_s of 24. Also, the number of outer stator armature winding pole pairs for all these machines is the same as p_s of 2. The relationships of the tooth-pole for the outer stator also obey the principles of the equations of (1)–(3).

III. Machine Analysis

A. Operation Principle Analysis

The proposed machines have double stators for accommodating two sets of 3-phase windings. So, they all offer six winding ends for different connections [1]. In general, the series and parallel connections between the winding ends in the same phases are the two common ways, which can respectively achieve the largest values of EMF and current. Here, the series connection way is adopted for obtaining the largest EMFs, which is shown in Fig. 2. It can be seen that the same phases of E_{A1} and E_{A2} are enlarged to E_A by vector overlay.

B. Electromagnetic Field Analysis

The time-stepping FEM (TS-FEM) is used to analyse the steady-state & transient performance of the proposed machines. The mathematical model consists of three set of equations. First, the electromagnetic field equation is governed by [10]:

$$\begin{cases} \Omega : \frac{\partial}{\partial x}\left(v\frac{\partial A}{\partial x}\right) + \frac{\partial}{\partial y}\left(v\frac{\partial A}{\partial y}\right) = -J - v\left(\frac{\partial B_{ry}}{\partial x} - \frac{\partial B_{rx}}{\partial y}\right) + \sigma\frac{\partial A}{\partial t} \\ S_1 : A_0 = 0 \end{cases} \tag{4}$$

where Ω is the field solution region, A the magnetic vector potential, J the current density, σ the electrical conductivity, and B_{rx}, B_{ry} the remnant flux density, along the x-axis and y-axis, respectively. Along the peripheries of outer stator and inner

TABLE I
MACHINE KEY DATA

Item	DSPMV	DSPMV-HTS	DSMG
Rated speed	200 rpm	200 rpm	200 rpm
Rotor outside diameter	228.0 mm	228.0 mm	228.0 mm
Rotor inside diameter	211.2 mm	211.2 mm	211.2 mm
Outer stator outside diameter	280.0 mm	280.0 mm	280.0 mm
Outer stator inside diameter	229.2 mm	229.2 mm	229.2 mm
Inner stator outside diameter	210.0 mm	210.0 mm	210.0 mm
Inner stator inside diameter	40.0 mm	40.0 mm	40.0 mm
Inner and outer airgap length	0.6 mm	0.6 mm	0.6 mm
Stack length	80.0 mm	80.0 mm	80.0 mm
(Note: The modulation-rings regarded as the stator part of the DSPMV-HTS.)			

stator at S_1, the magnetic vector potential A_0 is assumed to be zero. Second, the armature circuit equation is given as:

$$\frac{l}{S}\iint_{\Omega_e}\frac{\partial A}{\partial t}d\Omega = (R+R_l)i + (L_e+L_l)\frac{di}{dt} \tag{5}$$

where i is the stator phase current, R and L_e the resistance and inductance of the stator phase winding, R_l and L_l the resistance and inductance of the load, l the axial length of iron core, S the conductor area of each turn of per phase winding, and Ω_e the total cross-sectional area of conductors of each phase winding. Third, the movement equation is given by:

$$J_m\frac{d\omega}{dt} = T_e - T_L - \lambda\omega \tag{6}$$

where J_m is the moment of inertia, ω the mechanical speed, T_L the load torque, and λ the damping coefficient.

After coupling the equations of (4)–(6) and applying the discretization, the TS-FEM model is performed to deduce both the steady-state and dynamic performances of the machine. It should be noted that in this model for the DSMG machine, the permeability is set to zero, which stands for the flux-shielding effect of HTS bulks. Also, since the HTS bulks are located in the stationary component of the stator, they can be fabricated with a very short length of 3 mm in radial direction. In addition, the HTS bulks are based on the 2nd generation YBCO material, which can achieve the critical current density up to 10^4 $\mathrm{A/cm^2}$ under the temperature of 77 K [11].

IV. COMPARISON OF MACHINE PERFORMANCE

By using the TS-FEM, the steady-state and transient performances of the proposed three machines are compared and analysed. Table I shows the corresponding key design data.

First, the airgap flux density distributions of these machines are calculated and compared as shown in Fig. 3. It can be seen that all waveforms of the inner and outer aigap flux density have 22 pole pairs within 360 degree and correspond to the two pole pairs of the stator rotating field. Thus, it proves the propose machines achieve the effective flux-modulation ability. Also, it can be observed that the DSPMV-HTS one has the obviously highest flux density than the other types due to its HTS bulks. And the DSMG machine has the lowest flux density since its flux-modulation rings lead to more flux leakages than the other two machines. The corresponding EMFs are given in Fig. 4. It

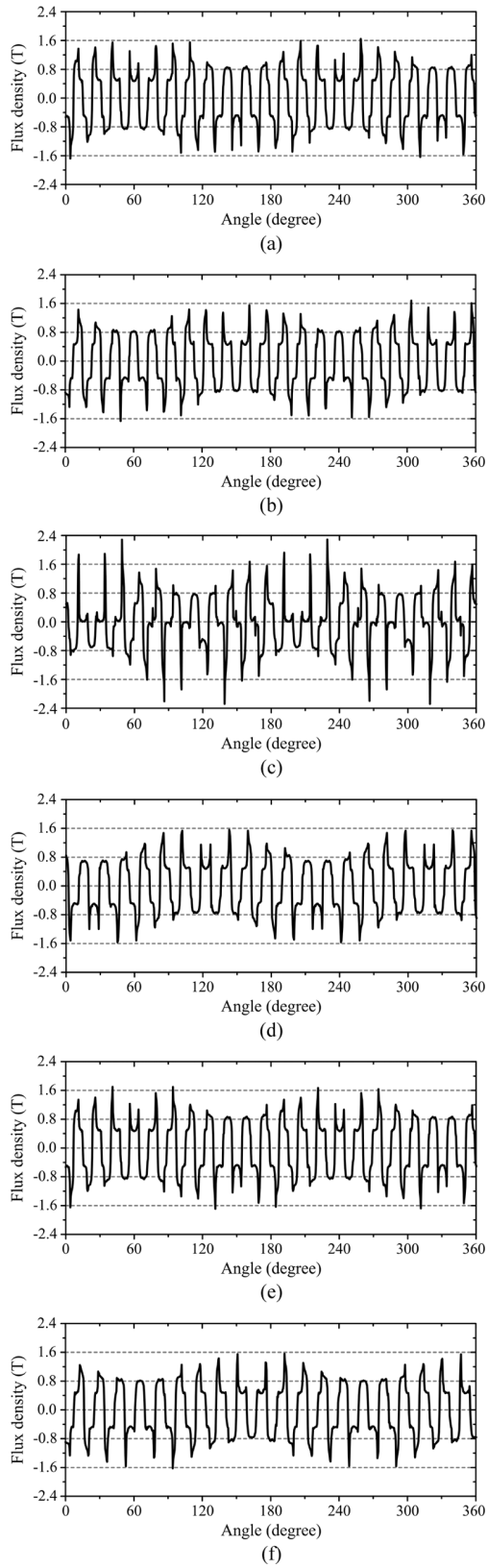

Fig. 3. Airgap flux density: (a) inner airgap of DSPMV machine, (b) outer airgap of DSPMV machine, (c) inner airgap of DSPMV-HTS machine, (d) outer airgap of DSPMV-HTS machine, (e) inner airgap of DSMG machine, and (f) outer airgap of DSMG machine.

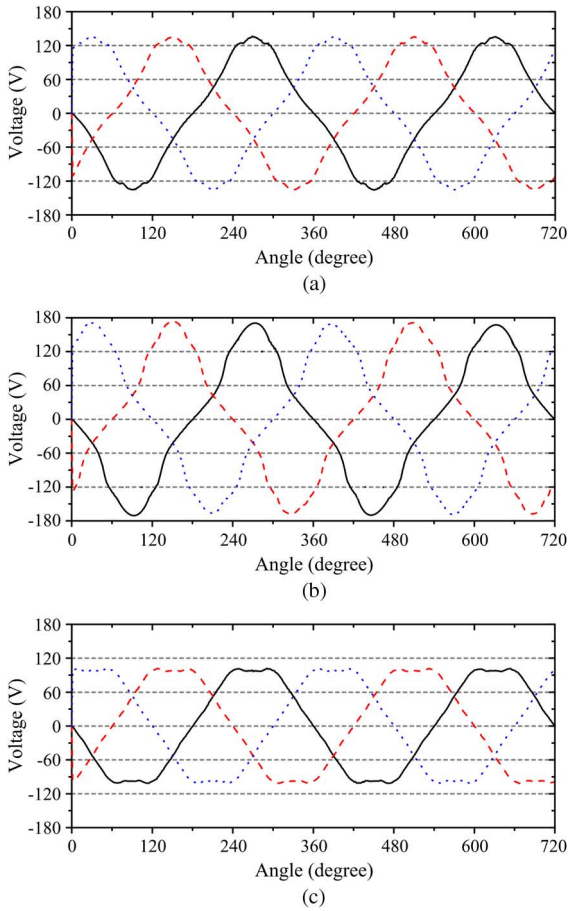

Fig. 4. No-load EMF waveforms at 200 rpm. (a) DSPMV machine, (b) DSPMV-HTS machine, and (c) DSMG machine.

also indicates the EMF amplitudes from the high to low are the DSPMV-HTS one, DSPMV one, and DSGM type.

Second, the torque performances of the machines are shown in Fig. 5. It can be found that the average steady torque (average cogging torque) of the DSPMV, DSPMV-HTS and DSGM machine is 65 Nm, 70 Nm and 58 Nm (4.2 Nm, 9.9 Nm & 4.5 Nm). Their cogging torque is significantly small, which are only 6.5%, 14.1% & 7.8% of their steady torque. In addition, the torque ripple is about 13.8%, 50.8% & 15.9%, respectively, which is also acceptable. The reason of the highest torque ripple and cogging torque for the DSPMV-HTS type is that the HTS bulks strengthen the flux distribution in stator yoke, which enlarges the un-balance of the airgap flux distribution.

Third, the core loss of these machines at rated load operation is compared in Fig. 6. As expected, the DSPMV-HTS type has the lowest core loss due to the HTS bulks enhancing the iron core effectiveness. Also, the DSMG machine has the highest core loss since its flux-modulation rings increase its power loss.

V. Conclusion

Based on the same peripherals of the outer and inner stators, stack length, and cup rotor, this paper quantitatively compares three flux-modulation machines, including the DSPMV

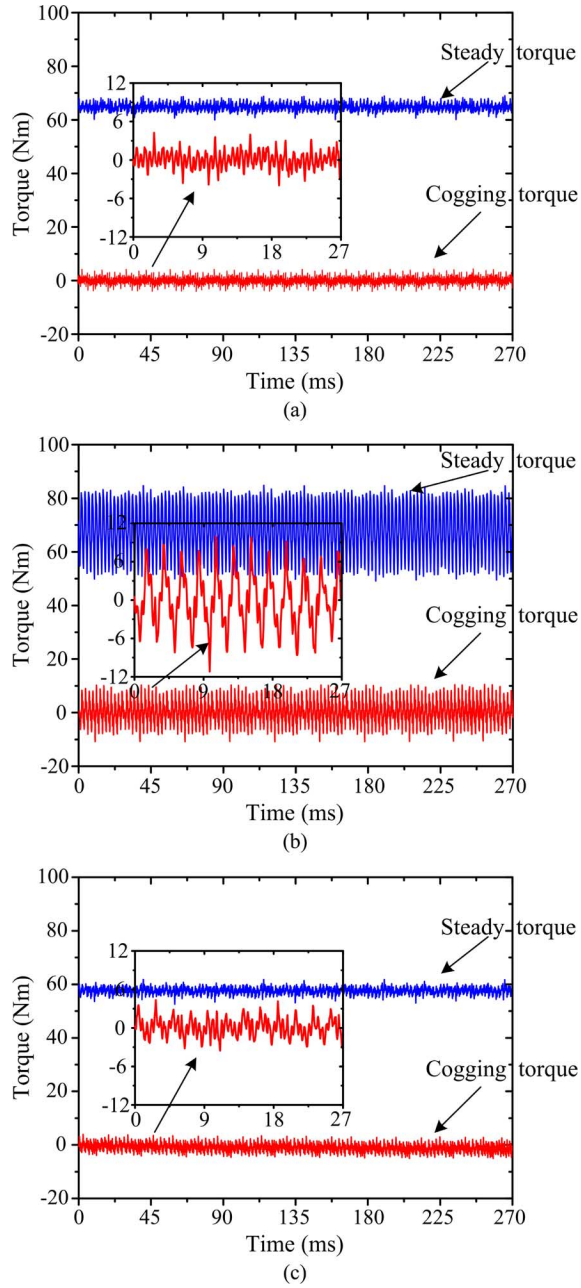

Fig. 5. Torque performance. (a) DSPMV, (b) DSPMV-HTS, and (c) DSMG.

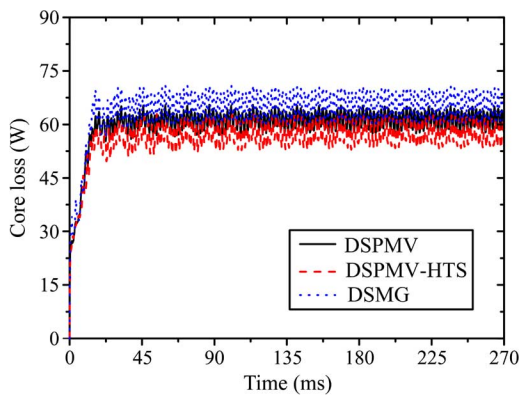

Fig. 6. Machine core loss at rated load operation.

TABLE II
MACHINE PERFORMANCE COMPARISON

Item	DSPMV	DSPMV-HTS	DSMG
Power	1360 W	1466 W	1215 W
RMS Inner airgap flux density	0.765 T	0.776 T	0.758 T
RMS Outer airgap flux density	0.745 T	0.752 T	0.736 T
EMF amplitude at 200rpm	136.5 V	141.9 V	102.0 V
Rated torque	65 Nm	70 Nm	58 Nm
Torque ripple at rated load	13.8%	50.8%	15.9%
Cogging torque amplitude	4.2 Nm	9.9 Nm	4.5 Nm
Cogging torque / rated torque	6.5%	14.1%	7.8%
Iron core loss at rated load	60 W	56 W	64 W

one, DSPMV-HTS one, and DSMG one. The comparison results are given in Table II, and concluded as follow.

1) All these machines achieve the effective flux modulation and hence produce the high torque at low speed operation.
2) The general performances of these machines can be ranked as: the DSPMV-HTS type, DSPMV type, and DSMG type.
3) The torque ripple and cogging torque of the DSPMV and DSMG machines are significantly small due to the multi-pole structure design. Although the counterparts for the DSPMV-HTS machine are the biggest ones, they're still acceptable for the practical application.
4) All these machines have the low iron core loss.

REFERENCES

[1] S. Niu, K. T. Chau, J. Z. Jiang, and C. Liu, "Design and control of a new double-stator cup-rotor permanent-magnet machine for wind power generation," *IEEE Trans. Magn.*, vol. 43, no. 6, pp. 2501–2503, Jun. 2007.

[2] A. Toba and T. A. Lipo, "Novel dual-excitation permanent magnet vernier machine," in *IEEE Ind. Appl. Conf. (IAS1999), 34th IAS Annual Meeting*, 1999, vol. 4, pp. 2539–2544.

[3] A. Toba and T. A. Lipo, "Generic torque-maximizing design methodology of surface permanent-magnet vernier machine," *IEEE Trans. Ind. Appl.*, vol. 36, no. 6, pp. 1539–1546, Nov. 2000.

[4] S. Niu, S. L. Ho, and W. N. Fu, "A novel direct-drive dual-structure permanent magnet machine," *IEEE Trans. Magn.*, vol. 46, no. 6, pp. 2036–2039, June 2010.

[5] K. Atallah, S. D. Calverley, and D. Howe, "Design, analysis and realization of a high-performance magnetic gear," *IEE Proc.-Electric Power Appl.*, vol. 151, no. 2, pp. 135–143, March 2004.

[6] K. T. Chau, D. Zhang, J. Z. Jiang, C. Liu, and Y. J. Zhang, "Design of a magnetic-geared outer-rotor permanent-magnet brushless motor for electric vehicles," *IEEE Trans. Magn.*, vol. 43, no. 6, pp. 2504–2506, June 2007.

[7] C. Liu, K. T. Chau, and W. Li, "Loss analysis of permanent magnet hybrid brushless machines with and without HTS field windings," *IEEE Trans. Appl. Supercond.*, vol. 20, no. 3, pp. 1077–1080, June 2010.

[8] J. Li and K. T. Chau, "A novel HTS PM vernier motor for direct-drive propulsion," *IEEE Trans. Appl. Supercond.*, vol. 21, no. 3, pp. 1175–1179, May 2011.

[9] C. Liu, K. T. Chau, and W. Li, "Design and analysis of a HTS brushless doubly-fed doubly-salient machine," *IEEE Trans. Appl. Supercond.*, vol. 21, no. 3, pp. 1119–1122, June 2011.

[10] C. Liu, K. T. Chau, and J. Z. Jiang, "A permanent-magnet hybrid brushless integrated-stater-generator for hybrid electric vehicle," *IEEE Trans. Ind. Electron.*, vol. 57, no. 12, pp. 4055–4064, Dec. 2010.

[11] B. H. Larsen, J. G. Larsen, A. B. Abrahamsen, H. F. Poulsen, T. Tschentscher, J. K. S. Christiansen, and N. H. Andersen, "Relation between texture and critical current density of textured YBa2Cu3Ox plates," *IEEE Trans. Appl. Supercond.*, vol. 11, no. 1, pp. 3513–3516, March 2001.